Chapter 2

Super-Reflection of light from a random amplifying medium with disordered complex refractive index

2.1 Introduction

The bosonic nature of light that allows for the possibility of phase coherent amplification/absorption of light gives rise to a new class of problems involving light propagation in a spatially random but coherently amplifying or absorbing media (RAM). As discussed in Section-1.5.1 of Chapter-1, this can lead to the phenomenon of mirrorless lasing in such active media and has been supported by the several experiments carried out on these systems [16, 86, 87, 88, 54]. However, the experimental findings of a narrowed spectral emission [16, 54] and a pulse narrowing of the emission [86, 88] above a well defined threshold of pumping could be explained merely as an effect of the long diffusive pathlengths in a random medium with gain (gain narrowing) and the consequent amplified spontaneous emission (ASE) [86, 89]. More recently, the observed super-narrowing of the emitted spectra from strongly scattering semi-conducting powder [60, 61] and from weak scatterers dispersed in high gain organic media [90] has been attributed to coherent feedback (distributed, but non-resonant), caused by recurrent multiple scattering [91].

In this chapter, we study the propagation of light and lasing in a random amplifying medium(RAM), specifically keeping in mind the coherent nature of the amplification. The spatial, temporal and spectral coherence of the laser light is essentially

due to stimulated emission, where the emitted photon has exactly the same phase, polarization and directionality as the incoming (stimulating) photon. This fact coupled with the coherent feedback offered by incipient Anderson localization of the light in a random medium makes us to expect new non-perturbative, synergetic effects, whereby the disorder induced localization of light enhances the amplification by confinement (essentially providing a virtual cavity), while the amplification increases the strength of localization by enhancing the coherent backscattering involving the longer return paths [55, 57, 58]. This enhanced folding manifests as the narrowing of the CBS cone at the central peak [87, 51]. In all these earlier studies, the active random medium is considered to scatter the propagating light (wave) due to fluctuations in the real part of the refractive index (η_r) (real potentials) while the coherent amplification is modelled by a phenomenological spatially constant imaginary part of the refractive index (η_i) (imaginary potential). Here we will study the case of a spatially fluctuating *imaginary* part of the refractive index. The case of a spatially fluctuating imaginary part of the refractive index, or potential is interesting in its own right, from the theoretical point of view and is necessary to realistically describe the experimental situation. In experiments [16, 88, 54, 53], where the scattering microparticles (e.g. polystyrene microspheres or titania rutile particles) are imbedded in a lasing medium, as the scattering particles are not active, a corresponding mismatch in the imaginary part of the refractive index is seen to exist. In other experiments [87, 86, 60, 61], where the microparticles (e.g. ZnO, GaN or Ti: Sapphire powder) are the active medium imbedded in a non-active polymer matrix or air, again a similiar mismatch is seen to exist. As it has been pointed out by Rubio and Kumar [92] a mismatch in the imaginary part of the refractive index (imaginary potential) would always cause a concomitant reflection (scattering) in addition to the absorption or amplification. Mismatch in η_i alone in an amplifying medium (negative imaginary potential) with no mismatch in η_r can cause resonant enhancement of the scattering coefficients. To make matters more clear, let us examine the one-dimensional case of a single δ-potential with complex strength $(V_R + iV_i)$ placed at the origin. Now, solving the Schrodinger equation for a plane wave incident on the potential from the left, we get for the transmission and reflection amplitudes:

$$T = \frac{1}{1 - \chi(V_r + iV_i)} \tag{2.1}$$

$$R = \frac{\chi(V_r + iV_i)}{1 - \chi(V_r + iV_i)} \qquad (2.2)$$

where $\chi = m/(i\hbar^2 k)$. As can be seen immediately, the reflection and the transmission coefficients can even diverge for a purely imaginary potential with $V_r = 0$ and $V_i = \chi^{-1}$ (corresponding to the case of amplification). This would correspond to the experimental situation where the scatterers (polystyrene microspheres, say) are suspended in a fluid with the same η_r (index matching fluid) in which a laser dye is dissolved and optically pumped. Thus, the mismatch in the imaginary part would be expected to have a much more drastic effect on the scattering than the mismatch in the real part. This makes it interesting to study the effect of the fluctuation in the imaginary part of the refractive index on Anderson localization and lasing in random media. Particularly, in the case of light, where extremely large scattering coefficients are necessary to cause Anderson localization [44], enhanced scattering due to mismatch in the imaginary part of the refractive index, i.e., amplification or absorption, can offer a novel mechanism for localization. The scattering caused by the fluctuations in η_i would, therefore be expected to have non-trivial effects on the wave propagation in the medium.

More specifically, we will investigate here the statistics of fluctuations of wave propagation in random media with quenched disorder in both the real and the imaginary parts of the refractive index. It is well known that the emergent quantities such as the reflection (or the transmission) from (or through) a disordered conductor are non-self-averaging quantities and a knowledge of the entire probability function of these quantities is required to describe the system. The transmittance across a randomly amplifying and absorbing chain was recently considered by Sen [93] numerically and was shown to decay exponentially with the increase in the length of the chain, presumably due to localization. But the effects of the fluctuation in the imaginary part of the refractive index on lasing in such random media has not been studied so far. In this work, we consider the statistics of the non-self-averaging fluctuations of the reflection coefficient for light incident on a one-dimensional active random medium with spatial correlated disorder in the imaginary part as well as the real part of the refractive index. A physical realization of interest here would be an Er^{3+} doped and pumped polarization maintaining optical fibre intentionally disordered along its length. The probability distribution of the reflection coefficient for light reflected

from a one-dimensional random amplifying medium with cross-correlated spatial disorder in the real and the imaginary parts of the refractive index is derived using the method of invariant imbedding. The statistics of fluctuations have been obtained for both the correlated telegraph noise and the Gaussian white-noise models for the disorder. In both cases, an enhanced backscattering (super-reflection with reflection coefficient greater than unity) results because of coherent feedback due to Anderson localization and coherent amplification in the medium. The results show that the effects of randomness in the imaginary part of the refractive index on localization and super-reflection are qualitatively different.

It is to be noted that our treatment is for a classical wave obeying the Maxwell equations. Thus, our results do not include the quantum statistical fluctuations of the electro-magnetic field. The light is taken to be in a coherent state, *viz.*, an eigenstate of the annihilation operator for the electromagnetic field with a large mean occupation number for a single photon mode.

2.2 Time-independent Maxwell's equations and amplifying media

The linear time-independent Maxwell's equation

$$\nabla^2 \vec{E}(\vec{r}) + \omega^2/c^2 \epsilon(\vec{r})\vec{E}(\vec{r}) = 0 \tag{2.3}$$

where $\vec{E}$ is the wave amplitude of the light wave, assumed to be time-harmonic with frequency w (and a scalar wave here for simplicity) and $\epsilon(\vec{R}) = \epsilon_r(\vec{r}) + i\epsilon_i(\vec{r})$ the complex dielectric constant, has been successfully used to describe a random amplifying media ($\epsilon_i < 0$) by several workers [55, 57, 58, 94, 63, 59, 93]. In these treatments one finds that the transmission through such media decreases with increasing amplification. This result appears counterintuitive as one would expect the amplification to aid propagation, and naively think that the transmission should increase with the amplification. Unlike the case of an absorbing medium, where the reduced transmission occurs trivially due to increased absorption, this result for amplifying media is thought to indicate an increase in the strength of localization due to increased probability of return of the wave amplitude through coherent backscattering involving long paths which now contribute more due to amplification. This effect has now become

well known as implying a symmetry between amplification and absorption [94, 49] and has been shown to hold in the case of the time-independent equation.

It is generally believed that the linear time-independent wave equation (TIWE) describes well the wave propagation in amplifying media for conditions corresponding to below-the-threshold of laser oscillation. Above the threshold, this linear equation is known to be inadequate for describing the actual lasing phenomenon as the coupling between radiation and matter is not properly accounted for. Recently, it has been argued by Soukoulis *et* al. [95], that that the TIWE and the associated stationary state scattering does not describe the situation above the threshold of lasing (oscillations) when the gain-length product exceeds criticality. In fact, their numerical result based on the time-dependent wave equation(TDWE) gives a transmission amplitude which grows exponentially in time.

We will now seek to understand the above result in the above-the-threshold paramater regime. In other words, the question we seek to answer is "What is the response of the system to a weak probe when the system can behave as an oscillator ?". Obviously for frequencies, when the (laser) resonance condition is satisfied (when $r_{21}r_{23}e^{2ikL} \geq 1$ and $kL = n\pi$, see below), the output diverges exponentially in time due to the onset of laser oscillations - the system is no longer an amplifier but becomes an oscillator. The exponential growth eventually tapers off due to non-linear processes such as saturation of the gain which are not considered here. However, for frequencies not satisfying the resonance condition of the cavity, the propagation(gain) at these frequencies in the cavity will be inhibited and the transmission should be attenuated.

To illustrate our point, we will consider a Fabry-Pérot setup (see Fig. 2.1) treated in Ref.[95] for ease of comparision. Thus we have a gain medium of length L between the facets with reflection coefficients r_{ij} and transmission coefficients t_{ij} respectively placed between two distant absorbers. The reflection and transmission coefficients at the facets are related to the complex wave-vector $k = k' + ik''$ (k" < 0 for the case of amplification) in the medium as (see Fig. 2.1) $r_{21} = r_{23} = (k - k_0)/(k + k_0) = R$, $t_{12} = 2k_0/(k + k_0)$, and $t_{23} = 2k/(k + k_0)$. where k_0 is the wave vector in free space outside the cavity. The TIWE can be solved easily for this case to yield a transmission
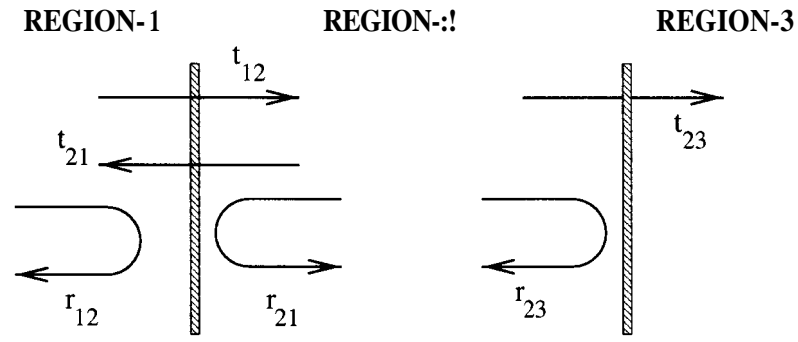
Figure 2.1: A schematic diagram of a Fabry-Pkrot etalon. The reflection and transmission (amplitude) coefficients for the facets are indicated.

amplitude

$$\mathcal{T} = \frac{t_{12}t_{23}e^{ikL}}{1 - r_{21}r_{23}e^{2ikL}},$$ (2.4)

which is well behaved for all frequencies and lengths except for $r_{21}r_{23}e^{2ikL} = 1$, which is the resonance condition. In fact, at large lengths, the Transmission is attenuated exponentially with length. The above result can also be obtained by using the method of partial waves caused by multiple scattering and summing the geometric series

$$\mathcal{T} = t_{12}t_{23}e^{ikL} \left[1 + r_{21}r_{23}e^{2ikL} + (r_{21}r_{23})^2 e^{4ikL} + \cdots \right],$$ (2.5)

where the first term represents the partial direct transmission of the incoming wave, the second term represents the partial wave reflected at the right facet then at the left facet before final transmission, and so on. Soukoulis et *al.* have argued that the above series can be summed only if $|r_{21}r_{23}e^{2ikL}| < 1$ and that the attenuated transmission at large lengths of the cavity is an artifact due to the assumption of a finite output in the TIWE. Consequently, they have concluded that the full TDWE has to be considered in order to describe the situation and have shown from a numerical calculation that such a treatment yields a transmitted wave amplitude that increases exponentially in time.

Now let us consider the exact solutions to the full time-dependent wave equation for the above case of the Fabry-Pkrot etalon. For the case of linear gain with no dispersion, an incident pulse propagates in the medium without changing its shape while undergoing amplification. Hence, the response function of the system for δ-pulse

incident from the left is

$$\mathcal{G}(t) = t_{12}t_{23}e^{\Delta}\delta(t - \tau) + t_{12}r_{23}r_{21}t_{23}e^{3\Delta}\delta(t - 3\tau) + t_{12}r_{23}r_{21}r_{23}r_{21}t_{23}e^{5\Delta}\delta(t - 5\tau) + \dots$$

(2.6)

where $\tau = L/c$, $\Delta = -k''c\tau$ the gain in one pass and c is the speed of propagation in the medium. It can be readily shown that for a time-harmonic wave $(e^{-i\omega t})$ incident at the first facet at time $t = 0$, the wave amplitude outside the second face at time t is given by,

$$\mathcal{T}(t) = t_{12}t_{23}e^{-(k''L - i\omega\tau)}e^{-i\omega t} \left[\frac{1}{1 - R^2 e^{-2(k''L - i\omega\tau)}} - \frac{\left(R^2 e^{-2(k''L - i\omega\tau)}\right)^{n+1}}{1 - R^2 e^{-2(k''L - i\omega\tau)}} \right], \quad (2.7)$$

where $n = Int[1/2(t/\tau - 1)]$ with Int denoting the integer value. It is seen that the first part on the right hand side is what we would get from a scattering treatment based on the TIWE, *i.e.,* as far as this term is concerned the expression obtained below threshold continues analytically in the expression obtained above the threshold. The second term on the right hand side, however, is what is not contained in this analytic continuation. It, indeed, gives the exponential growth of the transmitted amplitude (intensity) as in Ref.[95]. This growing oscillatory term (which may eventually get limited only by non-linearities not considered here) essentially is a noise imposed on the relatively weak transmission noted above. Further, rewriting the second part as

$$\frac{t_{12}t_{23}\exp[-2(k''L - i\omega\tau]\exp(i\phi)}{1 - r^2\exp[-2(k''L - i\omega\tau)]\exp(2i\phi)} \, r^{(t/\tau+1)}\exp[-k''L/\tau \, t]\exp[i\frac{\phi}{\tau} \, t], \quad (2.8)$$

where $R = r\exp(i\phi)$, we see that this exponentially growing part is at an effective frequency ϕ/τ. Note that this frequency is nothing but the rate of change of accumulated phase shift arising from multiple reflections at the interfaces, due to the mismatch in the imaginary part of the refractive index. The growing amplitude is extremely sensitive to the change in the parameters (e.g. R, T) of the system in the limit $t \to \infty$. Indeed, in principle, it is possible to pickup the small finite part referred to above as it is synchronous with the incident wave. The above exponential growth is at a different frequency and hence, not contained in the solutions of the TIWE which is essentially a harmonic analysis and only gives the Fourier component at the frequency of the incident wave. Hence we conclude that the treatments based

on the TIWE are, indeed, valid within the linear response theory and for the amplifying media as well. We have considered here the case of transmission for the ease of comparision with Ref.[95], but the case of reflection can be treated similarly. Of course, the above is a deterministic treatment that we have chosen for the purpose of illustration. For the random case, the interpretation has to be probabilistic.

2.3 Random amplifying medium with disordered complex refractive index

We consider a one-dimensional active disordered medium of length L with a random complex refractive index η, $0 \leq x \leq L$. For simplicity, polarization effects are neglected and light is assumed to be a scalar wave. Further, only the linear case of the gain/absorption being independent of the wave amplitude is considered and the non-linear features such as gain saturation are not considered. Here we would like to re-emphasize that our treatment is for the possibility of super-reflection ($r > 1$) i.e., for an amplifier and not an oscillator[1]. The complex wave amplitude $E(x)$ obeys the Helmhotz equation inside the medium,

$$\frac{d^2 E(x)}{dx^2} + k^2 \left[1 + \eta(x) \right] E(x) = 0, \tag{2.9}$$

where k is the wave vector in the medium ($k^2 = \omega^2 / c^2 \epsilon_0$) and $\eta(x) = \eta_r(x) + \imath [\bar{\eta}_i + \eta_i(x)]$ is the complex refractive index. Here $\eta_r(x)$ and $\eta_i(x)$ are random and $\bar{\eta}_i$ is a constant representing the average amplification or absorption in the medium according as $\bar{\eta}_i$ is negative or positive. It is well known that Eq.(2.9) can be transformed to give an equation for the evolution of the emergent quantity, namely, the complex amplitude reflection coefficient $R(L) = [r(L)]^{1/2} \exp[\imath \theta(L)]$ as a function of the sample length L, via the method of invariant imbedding [96, 97] (see Appendix-A) as

$$\frac{dR(L)}{dL} = 2ikR(L) + \frac{ik}{2}\eta(L)\left[1 + R(L)\right]^2. \tag{2.10}$$

Equation (2.10) is a stochastic differential equation and we are interested in the corresponding Fokker-Planck equation for the probability distribution $P(r, 6; L)$ which can be readily obtained following the standard procedures. Thus, let $\Pi(r, \theta; L)$ be the

---

[1]See the last part of Section. 1.5.1

density of points in the (r,θ) phase space. Now $\Pi(r, \theta; L)$ must satisfy the Stochastic Liouville equation [98],

$$\frac{\partial \Pi(r, \theta : L)}{\partial L} = -\frac{a}{\partial r} \left(r\Pi(r, \theta : L) \right) - \frac{\partial}{\partial \theta} \left(\theta\Pi(r, \theta : L) \right), \qquad (2.11)$$

and by the van Kampen lemma[98], the probability distribution function $P(r, \theta; L) = \langle \Pi(r, \theta; L) \rangle_{\eta_r, \eta_i}$, where the angular brackets denote averaging over all the realizations of the random refractive indices η_r and η_i.

2.3.1 The Gaussian 6-correlated (white-noise) disorder

First, let us consider the simplest case namely that of a Gaussian 6-correlated (white-noise) model. In this model, η_r and η_i are assumed to have 6 correlated Gaussian distributions with $\langle \eta_r(L) \rangle = 0$, $\langle \eta_i(L) \rangle = 0$, $\langle \eta_r(L)\eta_r(L') \rangle = \Delta_r^2 \delta(L - L')$ and $\langle \eta_i(L)\eta_i(L') \rangle = \Delta_i^2 \delta(L - L')$. This model would most appropriately describe the case of a continuous random medium such as a laser-dye doped gel or intralipid suspension [99], where the fluctuations in η_r and η_i are uncorrelated. Using the Novikov theorem [100] (See Appendix-B) to average over all configurations of η_r and η_i, we obtain in the random phase approximation (RPA) (*i.e.*, $P(r, \theta) = P(r)/2\pi$),

$$\frac{\partial P}{\partial l} = \phi_r \mathbf{L_R} P + \phi_i \mathbf{L_I} P + 2A \frac{\partial(rP)}{\partial r}, \qquad (2.12)$$

where the linear operators $\mathbf{L_R}$ and $\mathbf{L_I}$ are given by

$$\mathbf{L_R} = \frac{1}{2}\left[r(r - 1)^2 \frac{\partial^2}{\partial r^2} + (5r^2 - 6r + 1)\frac{\partial}{\partial r} + 2(2r - 1) \right], \qquad (2.13)$$

$$\mathbf{L_I} = \frac{1}{2}\left[r(r^2 + 10r + 1)\frac{\partial^2}{\partial r^2} + (5r^2 + 30r + 1)\frac{\partial}{\partial r} + 2(2r + 5) \right], \qquad (2.14)$$

and the non-dimensional sample length $1 = 1/2max\{\Delta_r^2, \Delta_i^2\}k^2 L \equiv L/l_c$, $\phi_r = \Delta_r^2/max\{\Delta_r^2, \Delta_i^2\}$, $\phi_i = \Delta_i^2/max\{\Delta_r^2, \Delta_i^2\}$ and $A = 2\bar{\eta}_i/max\{\Delta_r^2, \Delta_i^2\}k \equiv l_c/l_{amp}$ Here $l_{amp} = (\bar{\eta}_i k)^{-1}$ is the amplification length in the medium defined by the average of the imaginary part of the refractive index and max implies the superior value of the arguments. The RPA is known to be valid in the the weak disorder limit, $kl_c \gg 1$, where l_c is the localization length [97]. We point out that even if η_r and η_i were cross-correlated, the final equations do not differ in the RPA for the white-noise model (because $\langle \mathbf{L_1 L_2} P \rangle_\theta = 0$ see equations (2.19), (2.20).
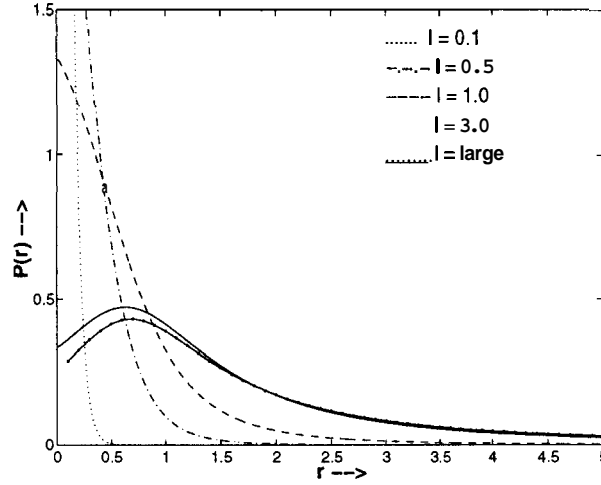
Figure 2.2: The probability distribution of reflectivity $P(r;l)$ in the case of the white-noise disorder given by eqn.(2.12), and the real disorder dominating ($\phi_r = 1.0$, $\phi_i = 0.1$), for the different sample lengths indicated. The line joining the dots is the analytic result for $P(r;\infty)$. The amplification parameter is A $= -0.25$.

The asymptotic $l \rightarrow \infty$ limiting solution of Equation.(2.12) obtained by setting $\partial P/\partial l = 0$ is given by,

$$P(r;\infty) = P_0\exp\left\{-2A/\gamma\tan^{-1}[((\phi_r+\phi_i)r+5\phi_i-\phi_r)/\gamma]\right\}$$
$$[(\phi_r+\phi_i)(1+r^2)+2(5\phi_i-\phi_r)r]$$

$$for \qquad\qquad \phi_r > 2\phi_i, \qquad\qquad (2.15)$$

$$= \frac{P_0}{(\phi_r+\phi_i)(1+r^2)+2(5\phi_i-\phi_r)r}\left[\frac{(\phi_r+\phi_i)r+5\phi_i-\phi_r-\gamma}{(\phi_r+\phi_i)r+5\phi_i-\phi_r+\gamma}\right]^{-A/\gamma}$$

$$for \qquad\qquad \phi_r, < 2\phi_i \qquad\qquad (2.16)$$

where $\gamma = \sqrt{12\phi_i|\phi_r - 2\phi_i|}$ and P_0 is a normalization constant given by $[\int_0^\infty P(r,\infty)dr]^{-1}$. The limit $l \rightarrow \infty$ implies physically L $>>$ l_c. This expression goes over straightforwardly to the result of Pradhan and Kumar[55] in the limiting case of pure real disorder ($\phi_i = 0$). Thus the statistics qualitatively differ in the two regimes for an amplifying medium : (i) when the real part of the disorder dominates ($\phi_r > 2\phi_i$) and (ii) when the imaginary part of the disorder dominates ($\phi_r < 2\phi_i$).

We have also solved equation(2.12) numerically for a finite length to investigate the approach to the asymptotic forms given by eq.(2.15). The parabolic differential equation(2.12) was solved by discretizing the equation and using a numerically stable implicit scheme [156]. In Fig. 2.2, the plots of $P(r,l)$ for the case of real disorder dominating ($\phi_r > 2\phi_i$) for different lengths of the medium are shown. The prob-
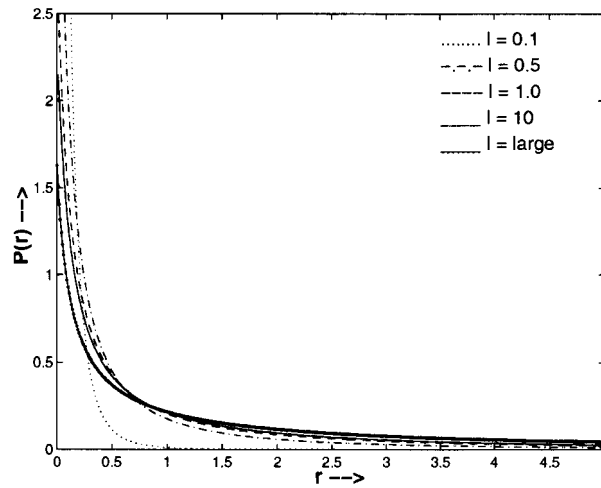
Figure 2.3: The probability distribution $P(r;l)$ in the case of the white-noise disorder given by eqn.(2.12), and a pure imaginary mismatch $(\phi_r = 0)$ for different lengths of the sample. The line joining the dots is the analytic result for $P(r;\infty)$. The amplification parameter is $A = -1$.

ability distribution for the case of a pure imaginary mismatch $(\phi_r = 0)$, with the real part η_r being index-matched is shown in Fig. 2.3. The line joining the dots in both the figures corresponds to the asymptotic $P(r;\infty)$ solution. In the case of amplifying medium, the value of reflectivity (r_{max}) at which $P(r;l)$ peaks increases with the average value of the amplification factor $|A|$. For the case of the imaginary part disorder dominating, $P(r;l)$ has a peak at small values of the reflectivity even for moderate values of the amplification. In the case of an absorbing medium with the imaginary disorder dominating, the probability distribution has a monotonic decreasing behaviour and is maximum at $r = 0$. A finite probability of reflection at $r > 1$ in the absorbing case and at $r < 1$ in the amplifying case $(A < 0)$ is recognized to be a consequence of the two-sidedness of the white-noise process for the complex refractive index, which allows the imaginary part of the refractive index $(\bar{\eta}_i + \eta_i)$ to take on locally both positive and negative values for any given value of the average. It should be noted that this limiting form of $P(r,\infty)$ gives a weak logarithmic divergence for (r) (for $\phi_i \neq 0$), regardless of the sign of A for both absorption and amplification. Thus, amplification has a much more drastic effect on the reflectivity than attenuation. The white-noise process allows the local fluctuations in η_i to be very large and the effect of a finite mean value $\bar{\eta}_i$ is small. It is thus a case of the

fluctuations dominating over the mean. We also find that the numerical solutions saturate to the limiting forms for $l \gtrsim 1$. So most of the reflection occurs from within a localization length. This enhanced backscattering is quite different from that caused by light diffusion[86, 89]. In the latter case, the distribution of optical path length, because of exponential growth of wave amplitude due to coherent amplification in one-dimension, gives $P^D(r; \infty) \sim \ln(r)^{1/2}/r$ for $r >> 1$. This decays much slower than the $P(r; \infty)$ for $r \rightarrow \infty$, as given by eq.(2.15).

2.3.2   Correlated telegraph disorder

In the case of the white-noise disorder, the imaginary part of the refractive index was allowed to take on both positive and negative values *i.e.,* the medium could be locally both amplifying or absorbing. With a view to studying purely amplifying/absorbing random media, we use the telegraph disorder model to describe the fluctutations in the refractive index. Moreover, since the gain/absorption coefficient is physically always bounded from above, the fluctuations in the imaginary part of the refractive index are better described by this dichotomic Markov process (i.e., spatial Telegraph noise). Further, we recognize that in discrete random media such as microparticles suspended in a laser dye solution used in experiments, the real and the imaginary parts of the refractive index fluctuate spatially in the same manner and can, therefore, be described by the same stochastic process. A telegraph noise with a finite correlation length is most appropriate to describe such a situation. Accordingly, we will choose $\eta_r(L) = \alpha \chi(L)$ and $\eta_i(L) = \beta \chi(L)$ with an average value for the imaginary part $\bar{\eta}_i$. Here $\chi(L)$ is taken to be a dichotomic Markov process which can take on the values $\pm \chi$ such that $\langle \chi(L) \rangle = 0$ and $\langle \chi(L) \chi(L') \rangle = \chi^2 \exp\left(-\Gamma|L - L'|\right)$, where Γ^{-1} is the correlation length in the medium.

Now, defining as before, $P(r, 8; L) = \langle \Pi(r, 8; L) \rangle_\chi$ and $W(r, 8; L) = \langle \chi(L) \Pi(r, 8; L) \rangle_\chi$, and using the "formulae of differentiation" of Shapiro and Loginov[101] (see Appendix-C) to average over the dichotomous configurations of $\chi(L)$, we obtain

$$\frac{\partial P}{\partial L} = -2k\frac{\partial P}{\partial \theta} + \bar{\eta}_i \mathbf{L_2} P + (\alpha \mathbf{L_1} + \beta \mathbf{L_2})W, \tag{2.17}$$

$$\frac{\partial W}{\partial L} = \chi^2(\alpha \mathbf{L_1} + \beta \mathbf{L_2})P - 2k\frac{\partial W}{\partial \theta} + \bar{\eta}_i \mathbf{L_2} W - \Gamma W, \tag{2.18}$$

where the linear operators $\mathbf{L_1}$ and $\mathbf{L_2}$ are :

$$\mathbf{L_1} = -k \left[\sin\theta \frac{\partial}{\partial r} \sqrt{r}(1-r) + \frac{\partial}{\partial\theta} + \frac{1}{2}\left(\sqrt{r} + \frac{1}{\sqrt{r}}\right)\frac{\partial}{\partial\theta}\cos\theta \right], \qquad (2.19)$$

$$\mathbf{L_2} = k \left[\cos\theta \frac{\partial}{\partial r} \sqrt{r}(1+r) + 2\frac{\partial}{\partial r}r + \frac{1}{2}\left(\sqrt{r} - \frac{1}{\sqrt{r}}\right)\frac{\partial}{\partial\theta}\sin\theta \right]. \qquad (2.20)$$

We thus get a closed system of equations for $P(r,\theta,\mathrm{L})$ and $\mathrm{W}(r,8,\mathrm{L})$. These equations go over correctly to the corresponding eq.(2.12) in the white-noise limit obtained by taking the limit $\chi^2 \to \infty$, $\Gamma \to \infty$ while keeping $\chi^2/\Gamma = \mathrm{A}^2$ constant. In this limit, the equation for $P(r,8;\mathrm{L})$ becomes autonomous *i.e.*, it gets decoupled from $\mathrm{W}(r,8;\mathrm{L})$.

In the RPA $\langle P\rangle_\theta = 0$ arid $\langle W\rangle_\theta = 0$, and in the asymptotic limit $\mathrm{L} \to oo$, these equations simplify to

$$\beta\bar{\eta}_i\mathbf{L_I}P + \alpha^2\mathbf{L_R}W + \beta^2\mathbf{L_I}W = 0 \quad , \qquad (2.21)$$

$$\alpha^2\mathbf{L_R}P + \beta^2\mathbf{L_I}P + 2A\frac{\partial(rP)}{\partial r} - \frac{\bar{\eta}_i\beta}{\chi^2}\mathbf{L_R}W = 0 . \qquad (2.22)$$

where $\mathbf{L_R}$ and $\mathbf{L_I}$ are given by eq.(2.13) and eq.(2.14) and $A = 2\Gamma\bar{\eta}_i/\chi^2$. Interestingly in the case of the pure real part disorder $(\beta = 0)$, the form of the telegraph noise equation for $P(r;\infty)$ is identical to that for the white- noise case, but with the coefficient $A = 2\Gamma\bar{\eta}_i/k\chi^2$. Similarly, in the case of the pure imaginary part disorder $(\mathrm{a}= 0)$, the form of the telegraph noise equation for $P(r;\infty)$ is again identical to that for the white-noise case, but with the coefficient $A = 2\Gamma\bar{\eta}_i/k(\chi^2 - \bar{\eta}_i{}^2)$. However, for $\beta\chi < |\bar{\eta}_i|$, the imaginary part of the refractive index is always positive (absorbing) or negative (amplifying). Hence the solution for these two cases is also given by eq.(2.15), the solutions being valid in the interval $0 < r < 1$ for the absorbing medium, and $1 < r < \infty$ for the amplifying medium. Outside the intervals, the probability density $P(r;\mathrm{L})$ vanishes.

A complete solution for the eq.(2.21)and eq.(2.22) is obtained as

$$
\begin{aligned}
P(r;\infty) &= P_0 \left[\frac{1}{\xi_+(1 + \zeta_+ r + r^2)} + \frac{1}{\xi_-(1 + \zeta_- r + r^2)} \right] \times \\
&\quad \times \quad \exp[-2A\left(I_+(r) + I_-(r)\right)], \qquad (2.23)\\
I_\pm(r) &= \frac{1}{\xi_\pm\sqrt{\zeta_\pm^2 - 4}} \ln\left| \frac{r - r_\pm^{(2)}}{r - r_\pm^{(1)}} \right| \qquad |\zeta_\pm| > 2,\\
&= \frac{1}{\xi_\pm\sqrt{\zeta_\pm^2 - 4}} \tan^{-1}\left(\frac{\zeta_\pm + 2r}{\sqrt{\zeta_\pm^2 - 4}} \right) \qquad |\zeta_\pm| < 2,
\end{aligned}
$$

where $\xi_\pm = a^2 + \beta^2 \pm \beta\bar{\eta}_i/\chi$, $\zeta_\pm = [10(\beta^2 \pm \beta\bar{\eta}_i/\chi) - 2\alpha^2]/[1 \pm \sqrt{\beta} + \alpha^2]$, $r_\pm^{(1)} = -1/2[\zeta_\pm + (\zeta_\pm^2 - 4)^{1/2}]$, $r_\pm^{(2)} = -1/2[\zeta_\pm - (\zeta_\pm^2 - 4)^{1/2}]$ and P_0 is a normalization coefficient. These expressions become the same as given by eqn.(2.15) in the white noise limit ($\chi^2 \to \infty$, $\Gamma \to \infty$ and χ^2/Γ being constant).

The solutions for one-sided disorder in the imaginary part exhibit three qualitatively different behaviours corresponding to choices of the parameters a, β and $\bar{\eta}_i$ (χ is an arbitrary constant and can be set to unity without loss of generality). First, we note that the case of $a^2 + \beta^2 - \beta|\bar{\eta}_i|/\chi = 0$, corresponds to a singular perturbation of the differential equation for $P(r;\infty)$. This condition can be interpreted as a threshold condition by noting that the localization length is given by $l_c^{-1} \sim (a^2 + \beta^2)$ and the effective amplification length is given by $l_{amp}^{-1} \sim \beta\bar{\eta}_i$. This condition then corresponds to a matching of length scales in the problem, $l_c = l_{amp}$. In the regime where the amplification dominates the localization ($a^2 + \beta^2 - \beta|\bar{\eta}_i| < 0$ or $l_c > l_{amp}$), the solutions exhibit a monotonic decreasing behaviour in the region of interest ($1 \le r < \infty$). Here the disorder in the real part (a) is small and does not affect the statistics appreciably, as can be seen from Fig. 2.4a. For ($a^2 + \beta^2 - \beta|\bar{\eta}_i| > 0$ or $l_c < l_{amp}$), a natural boundary arises for the solutions of the equation at $r_-^{(2)}$ which falls in the domain of physical interest ($1 \le r < \infty$). Now the solutions given by the expression(2.23) are valid in the range $r_-^{(2)} \le r < \infty$ with $P(r;\infty) = 0$ outside. In this regime the localization dominates ($1, < l_m$), if $2A/[\xi_-(\zeta_-^2 - 4)^{-1/2}] > 1$ and we have a broad distribution with peak at $r_{max} > r_-^{(2)}$ and $P(r_-^{(2)};\infty) = 0$ (Fig. 2.4b). The value of r_{max} is large for small disorder in the real part ($a^2 + \beta^2 - \beta|\bar{\eta}_i| \gtrsim 0$), and decreases as a increases. The behaviour in this region is dominated by the disorder in the real part of the refractive index. A third qualitatively different behaviour occurs for $1, < l$ and $2A/[\xi_-(\zeta_-^2 - 4)^{-1/2}] < 1$. Then the expression given by eqn.(2.23) diverges at $r_-^{(2)}$. This divergence is, however, normalizable implying that $P(r;\infty)$ is peaked (in fact, sharply) at that point. This behaviour can be readily understood by noting that the second condition which can be rewritten as $\bar{\eta}_i^2(\Gamma/k)^2 < 3\beta(|\bar{\eta}_i| - \beta)[a^2 + 2\beta(|\bar{\eta}_i| - \beta)]$, is basically a condition on the correlation length ($l_{corr} = \Gamma^{-1}$). This condition is satisfied for small Γ (large l_{corr}). Then the reflection is essentially from a single potential barrier and thus has a sharply defined value. It should be noted that, as $a \to \infty$, $P(r;\infty) \to \delta(r - 1)$, as expected.
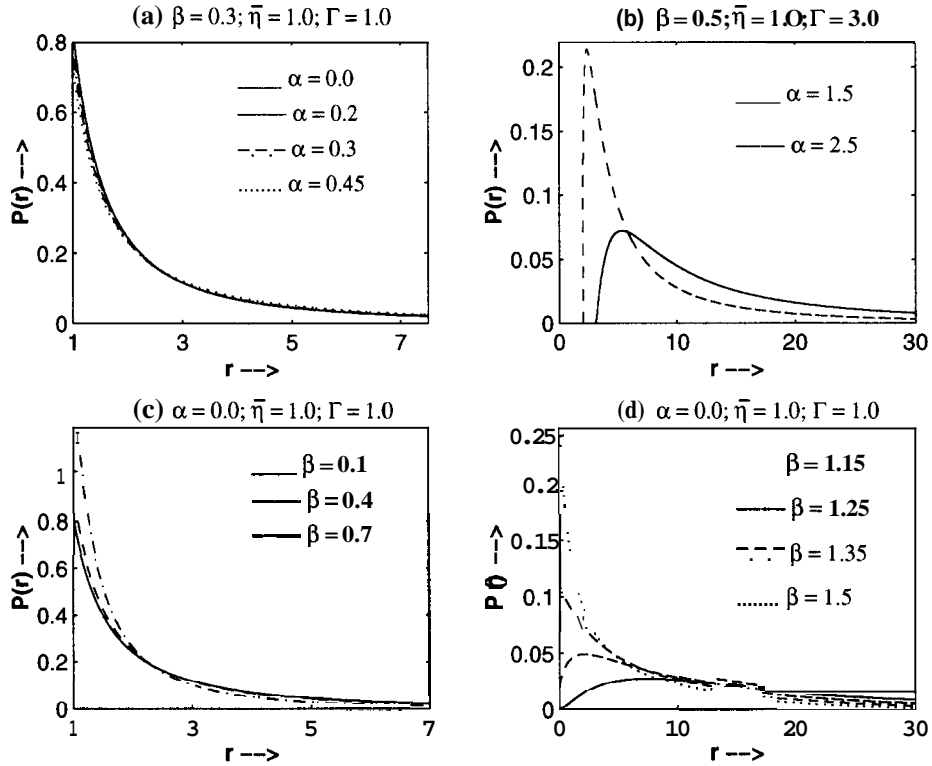
Figure 2.4: The probability distribution $P(r;l)$ in the case of the correlated telegraph noise. (a) $l_c > l_{amp}$ and (b) $l_c < l_{amp}$ are for one-sided disorder $(\beta < |\bar{\eta}_i|)$ with disorder in both the real and the imaginary parts. (c) $l, > l_{amp}$ and (d) $l_c < l_{amp}$ are for two-sided disorder $(\beta > |\bar{\eta}_i|)$ and pure imaginary mismatch (a $= 0$).

The solutions for the case of a two-sided disorder for the imaginary part $(\beta > |\bar{\eta}_i|)$ are similiar to the solutions for the white noise case. It should be noted that there does not exist real $r_-^{(2)}$ which falls into the physical region of interest $(0 \leq r < \infty)$. In this case the large disorder in the imaginary part (β) causes the effects of localization to dominate. However, in all cases of amplification, for a finite A and $a^2 + \beta^2 - \beta|\bar{\eta}_i| \neq 0$, there is a universal $1/r^2$ tail for the $P(r; \text{GO})$. For the case of pure imaginary disorder$(\alpha = 0)$, we similiarly see a monotonically decreasing behaviour of $P(r; \infty)$ with r for one-sided disorder $(\beta < |\bar{\eta}_i|$ or $l_c > l_{amp})$ (Fig. 2.4c), and a $P(r; \infty)$ with a peak for two-sided disorder $(\beta > |\bar{\eta}_i|$ or $l_c < l_{amp})$ (Fig. 2.4d). With increase in β for two-sided disorder, the peak shifts to smaller values of reflectivity as the effects of absorption show up, until for large enough β, the peaks occurs at $r = 0$ and we again have a monotonically decreasing $P(r; \text{GO})$. It should be mentioned that

all these effects are seen for the case of absorption also, with the roles of $r_-^{(1)}$ and $r_-^{(2)}$ interchanged.

2.4 Conclusions

In conclusion, we have studied the statistics of super-reflection from a one-dimensional disordered system with spatial randomness both in the real and the imaginary parts of the complex refractive index. We have discussed the models of disorder qualitatively applicable to experimental systems such as intentionally disordered optical fibres with gain (Er^{3+}-doped) and obtained the probability distribution function of the reflectivity for the cases of a white-noise disorder and a correlated telegraph disorder. In both cases, an enhanced reflection results because of coherent feedback due to Anderson localization and coherent amplification. In the case of white-noise disorder, the statistics are qualitatively different in the two regimes of the real part disorder dominating ($\Delta_r^2 > 2\Delta_i^2$) and the imaginary part disorder dominating ($\Delta_r^2 < 2\Delta_i^2$). In the case of telegraph disorder, we obtain three qualitatively different behaviours for $P(r; \infty)$ depending on threshold conditions involving the localization length, the amplification length and the correlation length. Thus the fluctuation in the imaginary part of the refractive index is seen to have a non-trivial and qualitatively different effect on localization and lasing from such random media.

Finally, it is to be noted that the domain of validity of our treatment and the results therefrom, for the super reflection from a random amplifying medium is restricted to operating conditions corresponding to below the threshold of lasing, *i.*e., to the parameter regime $l_c < l_{amp}$. Indeed the random amplifying medium operating in the reflection mode acts as a one-sided cavity of size l_c essentially open (hence leaking) in the direction of the incident beam (Of course, deep inside the medium, a photon injected, for example, through spontaneous emission will undergo indefinite amplification in an effectively closed cavity of size 1. Such an amplified spontaneous emission will lead to large storage of photons which will eventually be limited by non-linear effects in real systems). As l_c approaches l_{amp} from below ($l_c \lesssim l_{amp}$), the statistical weight for the reflection coefficient moves to higher values of reflectivity as indeed can be seen in Fig. 2.4b and Fig. 2.4d, and finally at $l_c > l_{amp}$, we would expect the random amplifier to become a random oscillator with self-sustaining os-

cillations at the eigenmodes of the system. Thus one may suspect the results for $l_1 > l_{amp}$ (Fig.2.4a and Fig.2.4c) to lie outside the validity of our treatment. We have shown in Section(2.2) that the treatment based on the TIWE is indeed valid to describe an amplifying system as well and hence, give an operational meaning (in the sense of a response to a probe at that frequency) to the results given by eqn.(2.23) in the above-the-threshold regime.

In our case, the imaginary potential not only causes the coherent amplification/absorption of the wave but also scatters the wave due to mismatch in the complex potential. It is to be noted that the amplification/absorption can also be modelled by using additional fake channels connected to reservoirs [49] or by stochastic amplification/absorption [102], where the amplification/absorption is introduced by an amplification/absorption constant per unit-length in the free propagation region between scatterers. In these cases, there will not be any extra scattering due to the amplification/absorption and the different cross-overs between the regimes of real disorder dominating or the imaginary disorder dominating in our case, might not carry over to the case of stochastic amplification/absorption. Here, we should perhaps point out that coherent amplification/absorption due to the imaginary potential is more applicable to the case of light, while the models of stochastic absorption are more applicable to electron (fermion) propagation.

Finally, as the phenomenon considered here is concerned with the issue of statistical fluctuations (noise) in a random amplifying medium, we propose for it the acronym RAMAN (Random Amplifying Medium And Noise).

Chapter 3

Correcting the quantum clock: The sojourn time in a scattering potential

3.1 Introduction

The time scales associated with the motion of a deformable object, such as a quantum-mechanical wave packet, scattered by a potential are operationally not context-free and raise some fundamental questions of interest for mesoscopic systems (for recent reviews see [67, 66, 68]). This is due essentially to the fact that for a deformable object in motion, there are no sharply defined starting and finishing lines, even classically! This problem is further accentuated for the case of quantum tunneling (evanescent waves), where the wave vector becomes imaginary and even the velocity of propagation is ill-defined. Thus, for example, the well known Wigner phase delay time [69], (defined in analogy with the problem of the group velocity) based on an identifiable fiducial feature, such as the peak of the wave packet, becomes meaningless under the conditions of strong distortion of the wave packet by the scattering potential[70, 103, 104]. Perhaps, the most striking manifestation of this feature is seen in the recent claims for superluminal propagation of a light pulse[66, 105].

One of the time scales relevant for many physical situations is what may be aptly called the sojourn time that literally measures the time of sojourn of a particle in the spatial region of interest, under given conditions of scattering. Clearly, this time must be positive definite. One can, of course, define the conditional sojourn times separately for the transmission and the reflection in the context of barrier crossing, e.g., we have the traversal (or tunneling) time for transmission through a barrier.

We could also generalize the sojourn time to include the dwell time for a particle initially prepared in a spatially confined state - this covers the decay time of a metastable state(see Section-1.6 for other possible time scales). The sojourn time is clearly distinct from the Wigner phase (ϕ) delay time, $\hbar\partial\phi/\partial E$, which can in fact, go negative. Operationally, the local sojourn time can be defined meaningfully by invoking a mathematical artifice called a "clock" involving attachment of an extra degree of freedom that co-evolves with the sojourning particle. Thus, we have the Larmor clock[76, 75] that involves the precessional angle accumulated by a spin associated with the particle in an infinitesimal magnetic field introduced for this purpose over the scattering locality of interest. Another 'clock' involves the time-harmonic modulation of the potential, and the timescale of traversal is identified with a certain (adiabatic to non-adiabatic) crossover phenomenon that occurs when the traversal time matches the period of modulation[70] (see Section-1.6.1 for details).

In this chapter, we will investigate yet another 'clock' (a 'non-unitary' clock), [79, 78, 106, 107] wherein the absorption/amplification caused by an infinitesimal imaginary potential formally introduced over the spatial region of interest, acts as a physical clock to 'count' the time of sojourn within the locality of interest. A rather subtle problem, however, associated with the 'non-unitary' clock, and possibly also with the Larmor clock, is that the very clock mechanism affects the sojourn time to be clocked finitely even as the perturbing clock potential is infinitesimally small ($V_i \to 0$ limit). This raises the question "Can the quantum-mechanical sojourn time be clocked without the clock affecting the sojourn time?". Thus, for instance, the conditional sojourn times calculated for certain non-random potential scatterers turns out to be negative. We recognise that the scattering concomitant with the mismatch, however weak, due to the very clock potential(iV_i) would affect the propagation of the wave in the sub-interval of interest. We propose a formal procedure by which the sojourn time can be clocked ideally using the non-unitary counter by correcting for these spurious scattering effects. The resulting sojourn time for traversal is then positive definite, has the proper high- and low-energy limits, and for a wide barrier goes over to the Biittiker-Landauer traversal time given by the Larmor clock. In the case of reflection, we find that the partial waves corresponding to the prompt part of the reflection have to be removed (suppressed) in order to obtain meaningfully a

positive sojourn time in the region of interest. This procedure is justified in that the partial waves corresponding to the prompt part of the reflection arising from the surface mismatch, would not have sampled the sub-interval of interest in order to get affected by the imaginary potential. In the case of a random potential, we find that the effects of the 'spurious' scatterings average out (due to the very random nature of the scattering) and hence, remains hidden. We have also worked out the delay times of reflection using the WKB approach, which suggests that the delay time for reflection is the same as the traversal time [73] within the WKB approximation.

3.2 Imaginary potential as a counter of sojourn time

The idea of the imaginary potential clock is simple and physically appealing. In the presence of an imaginary potential, a wave grows (or attenuates) exponentially. Thus, for an arbitrarily small imaginary potential, we expect that the sole effect of the imaginary potential would be that, the reflection or transmission coefficient becomes exponential with the time endured in the presence of the imaginary potential and thus, provides a natural counter for the sojourn time. Mathematically, the Schrodinger equation for the wave function $\psi(\vec{r}, t)$ of a particle in the presence of an imaginary potential is

$$i\hbar \frac{\partial \psi}{\partial t} = -\frac{\hbar^2}{2m} \nabla^2 \psi + [V_r(\vec{r}) + iV_i]\psi \tag{3.1}$$

can be transformed to a Schrodinger equation without the imaginary potential for the function $\phi(\vec{r}, t) = \exp(-V_i t/\hbar)\psi(\vec{r}, t)$. Hence, we write for the stationary (time-independent) case, $|\psi(\vec{r})|^2 = \exp(2V_i \tau_{vi}/\hbar)|\psi(\vec{r})|^2$, and interpret τ_{vi} as the time of sojourn in the sub-region where the imaginary potential is present. Now, we will further intuitively define the conditional sojourn times for the reflected and transmitted waves (in 1-D) as:

$$\tau_{vi}^R = \frac{\hbar}{2} \lim_{V_i \to 0} \frac{\partial \ln |R|^2}{\partial V_i}, \tag{3.2}$$

$$\tau_{vi}^T = \frac{\hbar}{2} \lim_{V_i \to 0} \frac{\partial \ln |T|^2}{\partial V_i}, \tag{3.3}$$

where $|R|^2$ and $|T|^2$ are the reflection and transmission probabilities respectively in the presence of the imaginary potential iV_i. In the limit $V_i \to 0$, the imaginary

potential was expected not to affect the dynamics of the wave propagation. In this approach, the local dwell time in any part of the scattering potential can also be calculated, by applying the infinitesimal imaginary potential only over that region of space. It is to emphasized here that the growth or attenuation of the wave is still a classical concept, but it is such an "irreducible" concept, that it is difficult to doubt its physical significance even at the risk of appearing naively realistic.

3.2.1 The average dwell time

Let us now consider the reflection and transmission from an arbitrary real potential with an added spatially constant imaginary potential (in 1-D). In the stationary case, the Schrodinger equation for the wavefunction ψ yields an identity

$$\frac{2V_i}{\hbar} \int_0^L |\psi|^2 dx = \frac{\hbar}{2im} \left[\psi^* \frac{\partial \psi}{\partial x} - \psi \frac{\partial \psi^*}{\partial x} \right]_0^L \tag{3.4}$$

where $[\ ]_0^L$ indicates the difference of the quantity within the brackets evaluated at L and 0 respectively. This yields that the sum of the reflection and transmission is greater (lesser) than unity for an amplifying (absorptive) potential. We can further write that

$$|T(V_i = 0)|^2 \tau_{vi}^T + |R(V_i = 0)|^2 \tau_{vi}^R = \frac{1}{c_g} \int_0^L |\psi(x)|^2 dx = \tau_d \tag{3.5}$$

where τ_d is the average dwell time defined earlier and is positive definite. Note that in the case of equal reflection and transmission times, they become equal to the average dwell time as well. This can be generalized in a straight-forward manner to the case of multi-channels and higher dimensions. This time has been claimed to represent the actual time of dwell [74, 68]. This quantity, however, scales differently at low energies (sub-barrier energies) compared to timescales obtained by other methods such as the Larmor clock [75].

3.2.2 The case of unitary reflection

It follows from the previous discussion that the sojourn time for reflection is positive definite in the case of unitary reflection ($|R| = 1$). In this case, it can be literally interpreted as the time of sojourn in the region. Further an interesting relationship between this dwell time and the Wigner phase delay time arises due to the analytic

properties of the S-matrix, corresponding to unitary wave reflection. The S-matrix in this case is simply the complex <u>amplitude</u> reflection coefficient, $R(E) = \exp[i\theta(E)]$ with $|R|^2 = 1$ for real E. Now from the analyticity of the S-matrix in the complex energy plane, we have $\partial(Re\ \theta)/\partial(Re\ E) = \partial(Im\ \theta)/\partial(Im\ E)$, where Re and I m denote the real and the imaginary parts respectively. As we approach the real axis, *i.e.*, in the limit $ImE \to 0$, we have $\partial(Re\ \theta)/\partial(Re\ E) = T/\hbar$ (Wigner time delay), while $\partial(Im\ \theta)/\partial(Im\ E) \to I m\ \theta/V_i$ as $V_i \to 0$ (along with I m θ). Thus we have $|R|^2 = \exp[2V_iT/\hbar]$ giving $|R|^2 - 1 = 2V_iT/\hbar$ in the limit $V_i \to 0$ (the latter corresponds to treating our electronic problem as a limit of vanishing imaginary part of the scattering potential).

It is to be noted that in the above, the variation of V_i was assumed to be global, *i.e.*, over the entire space $(-\infty, \infty)$, as is the variation in the wave energy (E). However, the imaginary potential is applied only locally within the region of interest in our proposal for the non-unitary clock. The two times are not strictly equal. The non-Unitary clock acts as a local clock compared to the Wigenr phase delay time which is a global quantity. From the Feynman path integral point of view, the particle (virtual) paths could go several times in and out of the region of interest (see Fig. 3.1). The imaginary potential amplifies/absorbs locally only the part of the

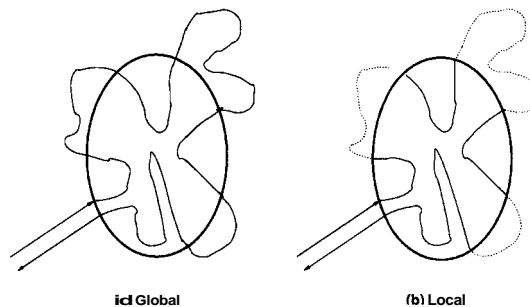**icl Global**   **(b) Local**

Figure 3.1: A schematic diagram showing a possible trajectory in the Feynman path integral sense. (a) shows the portion affected by a global variation of the potential and (b) shows the portion (solid line) affected by a local variation of the potential. The dotted portion of the trajectory is not counted.

path which lies within the region of interest. Hence, it can be taken to count only when the particle is inside the region. The variation of wave energy is by comparison global. It affects all parts of the path (inside as well as outside the region).
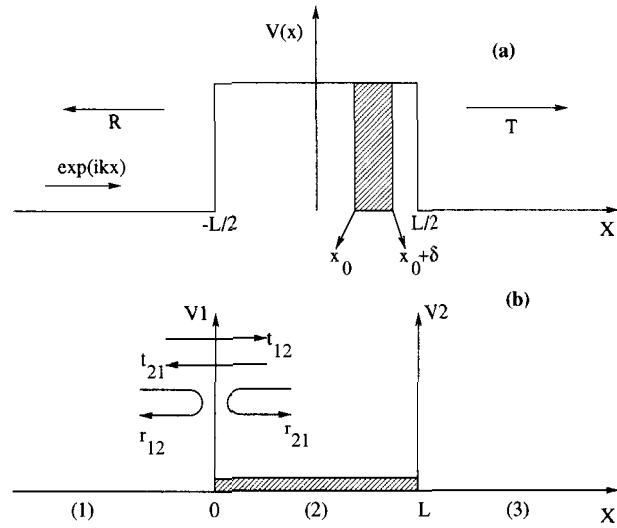
Figure 3.2: The potentials considered here (a)The rectangular barrier and (b)The δ-dimer. The hatched region indicates the presence of the clock potential (iV_i).

3.2.3   Negativity of the conditional sojourn times

Though the average dwell times is positive definite, there is no such restriction on the conditional sojourn times, which can be positive or negative. Indeed, it turns out that the conditional sojourn times calculated as defined above, can become negative for certain deterministic potentials. For example, an absorptive potential can increase the transmission, instead of reducing it - a manifestation of the Borrman effect in the context of X-ray scattering [108]. Below, we will consider the one-dimensional case with two output channels for a rectangular barrier and a 6 dimer (two δ-potentials separated by a spatial interval; see Fig. 3.2) and explicitly verify that the conditional sojourn times, indeed, go negative.

We calculate the reflection and the transmission coefficients for a plane wave of energy(E) incident on the barrier, by solving the Schrodinger equation (in the presence of iV_i, the clock potential) in each case and obtain the following results. The sojourn time in the entire barrier $\tau_s^{R,T}$, defined as above, for reflection(R) / transmission(T) for the case of the rectangular barrier of height (V_r) and thickness L is

$$\frac{\tau_s^{T,R}}{\tau_{BL}} = \frac{2(2 - v_r)p - v_r/kL \quad \sin(2pkL)}{4 - 4v_r + v_r^2 \sin^2(\mathrm{pkL})}, \tag{3.6}$$

where $p = \sqrt{1 - v_r}$, $v_r = V_r/E$, $\tau_{BL} = mL/\hbar k \sqrt{|v_r - 1|}$ (the Büttiker-Landauer time)

and $k = \sqrt{2mE}/\hbar$. These reflection and transmission sojourn times are equal, and equal to the average Smith dwell time. Thus, the imaginary potential was thought to be incapable of distinguishing reflection/transmission. The ratio $\tau_s^{T,R}/\tau_{BL}$, however, tends to zero for barrier penetration in the low-energy limit, and thus, does not give the proper low-energy limit[70]. We note though, that the sojourn time, so calculated, remains positive for this particular case. However, when we proceed to calculate the local dwell time in any given sub-interval of the rectangular barrier (e.g. in $(x_0, x_0+\delta)$, see Fig. 3.2a), we obtain different sojourn times for transmission and for reflection

$$\frac{\tau_s^T}{\tau_{BL}} = \frac{2(2 - v_r)p - 2v_r/k\delta \ \sin(pk\delta)\cos[pk(2x_0 + \delta)]\cos(pkL)}{4 - 4v_r + v_r^2 \sin^2(pkL)}, \quad (3.7)$$

$$\frac{\tau_s^R}{\tau_{BL}} = \frac{\tau_s^T}{\tau_{BL}} - \left\{ \frac{\sin[pk(2x_0 + \delta)]\sin(pk\delta)}{v_r p \sin(pkL)} \right\} \quad (3.8)$$

We check that these expressions correctly go over to those for the entire barrier when $x_0 = -L/2$ and $\delta = L$. In this case, $\tau_s^T = \tau_s^R$ when $x_0 = -\delta/2$, i.e., when the region we are interested in is symmetric about the center of the potential. But importantly, we note that τ_s^R can now become negative, and can even have negative (and positive) divergences at the resonances of the barrier (for $pkL = n\pi$). We note that the local sojourn times in different parts of the barrier add up (in spite of negativity etc.) to yield a positive sojourn time in the entire barrier.

Similarly, we obtain the sojourn times for the transmission and the reflection from the 6-dimer potential as

$$\tau_s^T = \frac{\hbar}{2E} \left\{ \frac{2(\beta_1 + \beta_2) \ \sin^2(kL) + [4 + (\beta_1^2 + \beta_2^2)]kL - (\beta_1^2 + \beta_2^2) \ \sin(kL)\cos(kL)}{[4 + (\beta_1 + \beta_2)^2 + \beta_1\beta_2(\beta_1\beta_2 - 4) \ \sin^2(kL) + \beta_1\beta_2(\beta_1 + \beta_2) \ \sin(2kL)} \right\}$$
$$(3.9)$$

$$\tau_s^R = \tau_s^T - \frac{\hbar}{2E}(\beta_1 - \beta_2) \left\{ \frac{(\beta_1 + \beta_2)[kL + \sin(kL)\cos(kL)] + 2\cos^2(kL)}{(\beta_1 - \beta_2)^2 \ \cos^2(kL) + [\beta_1\beta_2 \ \cos(kL) - (\beta_1 + \beta_2) \ \sin(kL)]^2} \right\}$$
$$(3.10)$$

where $\beta_{1,2} = 2mV_{1,2}/k\hbar^2$. We note that τ_s^T and τ_s^R are now different in general, and are equal only for $\beta_1 = \beta_2$ (the symmetric 6-dimer). Again, we observe that the sojourn times for reflection so obtained can become negative. Unlike the phase delay time which only compares the arrival of the peak in the presence of the potential to the potential-free case and is allowed to go negative, the negativity of the sojourn time (which is more like an interaction time) is clearly unacceptable.

3.3 Correcting the 'non-unitary' clock

In the following, we will trace this 'unphysical' feature to the 'spurious' scattering concomitant with the very clock potential (iV_i). We will first consider the case of transmission for the above-the-barrier wave energy(non-tunneling) and sub-barrier wave energy (tunneling) separately. The case of reflection where a further refinement of our proposal was required will be considered separately later.

3.3.1 The case of propagation (non-tunneling)

Let us first consider the case of propagation (non-tunneling), i.e., the wave energy to be above the barrier $(E > V_r)$. For this, we calculate the transmission and reflection amplitudes using the method of partial waves by multiple reflections arising from the interfaces of the rectangular barrier (See Fig. 3.2). In the case of propagation we obtain [47]

$$T = t_{12}t_{23}e^{ik'L} + t_{12}r_{23}r_{21}t_{23}e^{3ik'L} + t_{12}r_{23}r_{21}r_{23}r_{21}t_{23}e^{5ik'L} + \cdots \quad , \quad (3.11)$$

$$R = r_{12} + t_{12}r_{23}t_{21}e^{2ik'L} + t_{12}r_{23}r_{21}r_{23}t_{21}e^{4ik'L} + \cdots \quad , \quad (3.12)$$

where $k' = \sqrt{2m(E - V_r - iV_i)}/\hbar$ and, r_{12}, r_{23}, r_{21} and t_{12}, t_{23}, t_{21} are the reflection and the transmission amplitudes at the interfaces respectively (See Fig. 3.2). The transmission coefficient has a generic form $T = \sum_k A_k e^{i\phi_k} e^{\alpha_k L}$, where A_k, ϕ_k and α_k are real numbers representing the amplitude, phase and the growth of the partial waves. Consider, now, the sojourn time associated with this quantity

$$\tau_s^T = \lim_{V_i \to 0} \frac{\hbar}{2E} \frac{1}{|T|^2} \frac{\partial}{\partial V_i} \Big[\sum_k A_k^2 e^{2\alpha_k L} + \sum_{k \neq l} A_k A_l e^{i(\phi_k - \phi_l)} e^{(\alpha_k + \alpha_l)L} \Big]. \quad (3.13)$$

The imaginary part iV_i of the clock potential modifies the reflection / transmission coefficients (r_{jk}, t_{jk}) at the interfaces, where there is mismatch due to the imaginary clock potential. Now, the derivative with respect to the imaginary potential would cause terms of first order in V_i to contribute to $\tau_s^{T,R}$, even in the limit of an infinitesimal potential $V_i \to 0$. Thus, the counter modifies 'spuriously' the propagation of the wave itself in a non-trivial manner, in addition to the amplification or attenuation of the wave, for which it was introduced.

This analysis immediately suggests the key to correct the 'quantum clock' for the 'spurious' scattering. The whole point is that the presence of the imaginary potential

modifies the reflection and transmission coefficients at any point where the imaginary potential changes abruptly. We have to, therefore, devise a method by which the clock potential (iV_i) causes only the intended effect (amplification/absorption) without causing the 'spurious' scattering, i.e., it must be well apodized. A little thought of the perturbative structure of the scattering processes should convince one that the clock related growth/attenuation would only involve the paired combination $V_i\Delta$ (A being the spatial interval of interest) while the 'spurious' scattering would involve unpaired V_i. This motivates the following formal procedure to eliminate the 'spurious' effects. Treating V_i and $V_i\Delta = \xi$ as independent variables, we keep ξ formally constant and let $V_i \to 0$ in the expression for T. The sojourn time is now obtained as

$$\tau_s^T = \hbar\Delta/2 \lim_{\xi\to 0} \partial \ln |T(V_i=0,\xi)|^2/\partial\xi. \tag{3.14}$$

The same result is obtained by considering transfer matrices that explicitly suppress the 'spurious' scattering due to the clock potential iV_i.

Using either of the procedures, the sojourn times for the rectangular barrier can now be calculated. Thus, in the case of propagation $(v_r < 1)$, we have

$$\frac{\tau_s^T}{\tau_{BL}} = \frac{(1-|r_{21}r_{23}|^2)}{1+|r_{21}r_{23}|^2 - 2\Re(r_{21}r_{23}e^{2ik_rL})}, \tag{3.15}$$

where $\Re$ is the real part, $k_r = \sqrt{2m(E-V_r)}/\hbar$, and the r_{jk} and t_{jk} are the scattering amplitudes as before but with $V_i = 0$. We note that since $|r_{jk}| < 1$ for any real potential, the above sojourn time for transmission is always positive. For the case of the symmetric rectangular barrier $[r_{21} = r_{23} = (k - k_r)/(k + k_r)]$, the transmission and reflection sojourn times are equal and we explicitly obtain,

$$\frac{\tau_s^{T,R}}{\tau_{BL}} = \frac{2(2-v_r)p}{4 - 4v_r + v_r^2\sin^2(pkL)}, \tag{3.16}$$

where $p = \sqrt{1-v_r}$. We show plots of the sojourn time of transmission in a rectangular symmetric barrier and the S-dimer as a function of the potential strength in Fig. **3.3** (for v, < 1).

We note that the expression given by equation (3.15) is a general expression for a general class of problems. This is because the r_{jk} can be the scattering matrices for any arbitrary potential, with the only condition that the real potential within the sub-interval, where we seek the time of sojourn, should be constant (see Fig. 3.4).
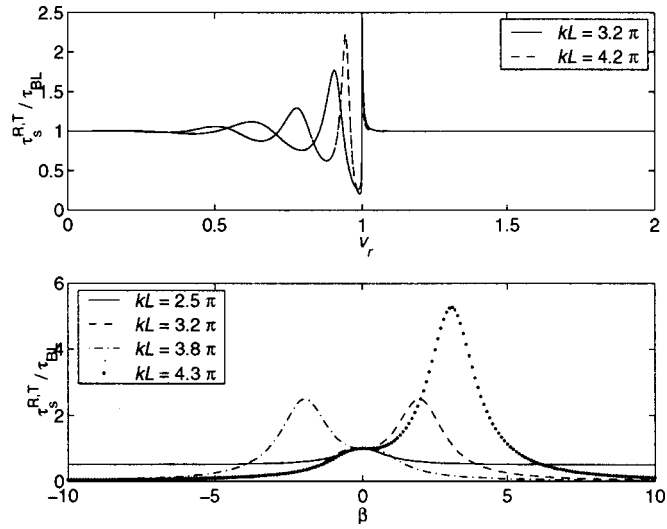
Figure **3.3:** The corrected sojourn times for transmission versus (a) $v_r = V_r/E$ for the rectangular barrier and (b) $\beta = 2mV/k\hbar$ for the symmetric 6- dimer. The times are normalized with respect to the Büttiker-Landauer traversal times (τ_{BL}).

This is, however, not a real restriction as it can be straight-forwardly verified that the local sojourn times for traversal in different parts of the potential add up to give the total sojourn time (a schematic is shown in Fig. 3.4b). Since any arbitrary potential can be constructed out of piece-wise constant potentials (in the limit of the width going to zero), we realize that the sojourn time for transmission given by this procedure is positive definite for any arbitrary potential.

3.3.2 The case of wave tunneling

For the case of tunneling (energies below the barrier energy $E < V_r$), we note that the wave vector becomes imaginary within the barrier. The real part of the potential sets its own length scale for the exponential decay / growth with distance inside the barrier. Essentially the roles of the real part and the imaginary part of the potential get interchanged. The imaginary part to first order in V_i causes an oscillation of the wave function with distance. Thus, the paired combination $\xi = V_i\Delta$, would affect the phase of the wave, rather than the amplitude. Mathematically, we are unable to analytically continue the expressions for propagation, i.e., for $v_r < 1$, to the case of tunneling (v, > 1). This is due to the fact that in determining the complex wave vector, we used an expansion where we assumed $v_i/|1 - v_r| \ll 1$. In the limit of an
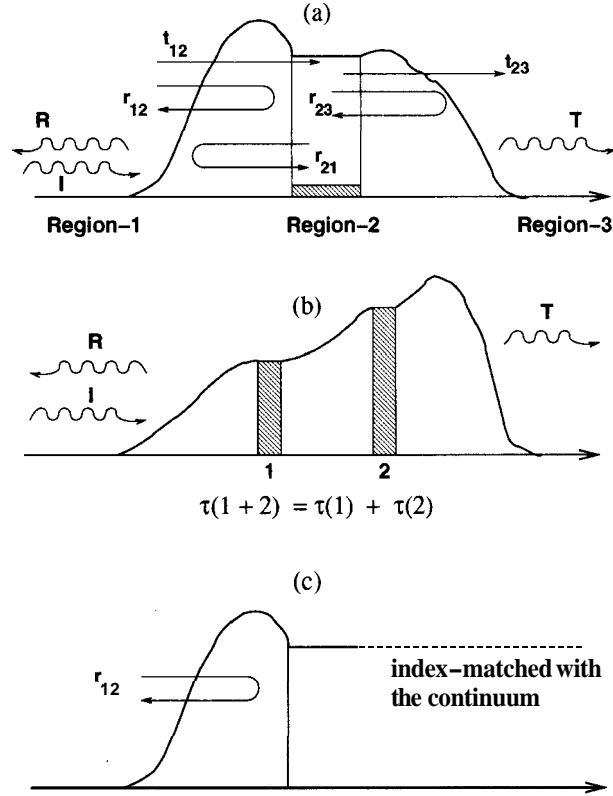
Figure 3.4: The general potential considered here (a)The region of interest is bounded by two arbitrary potentials whose scattering matrices are shown and (b) Shows two such regions, the local sojourn times of which add up to give the total sojourn time. The hatched region indicates the presence of the clock potential (iV_i). (c) The modified potential of (a), index matched to the continuum on the right from Region-2 onwards to have a reflection amplitude r_{12}.

infinitesimal v_i, this is true everywhere except at $v_r = 1$. Thus, there is a branch cut at $E = V_r$ in the complex energy plane. Indeed, if we analytically continue the expression for the traversal time in Eq. (3.15) to the case of tunneling, we would obtain a sojourn time which could be positive (v, > 2) or negative $(1 < v_r < 2)$.

Motivated by the success of using the paired combination for the case of propagation, we will define the sojourn time for transmission in the case of tunneling as the derivative of the phase with respect to the paired combination $\xi = V_i \Delta$:

$$\tau_s^T(v_r > 1) = i\hbar\Delta/2 \lim_{\xi \to 0} \frac{\partial}{\partial \xi} \ln[T(V_i = 0, \xi)/T^*(V_i = 0, \xi)] \qquad (3.17)$$

For the general case of Fig. 3.4a, we obtain the sojourn time of traversal as

$$\frac{\tau_s^T}{\tau_{BL}} = \frac{\left(1 - |r_{21}r_{23}|^2 e^{-4k_r L}\right)}{1 + |r_{21}r_{23}|^2 e^{-4k_r L} - 2\Re(r_{21}r_{23})e^{-2k_r L}}, \qquad (3.18)$$

where $k_r = \sqrt{2m(V_r - E)}/\hbar$ now. We note that this traversal time is positive definite for any arbitrary potential. Further, as before, the local sojourn times in different parts of the potential add up to give the total dwell time. For the case of the rectangular barrier we obtain

$$\frac{\tau_s^{T,R}}{\tau_{BL}} = \frac{(1 - e^{-4k_r L})}{1 + e^{-4k_r L} - 2[1 - 8(v_r - 1)/v_r^2]e^{-2k_r L}}. \tag{3.19}$$

The sojourn time is plotted in Fig. 3.3 (for v, > 1). For an opaque barrier ($L \gg k_r^{-1}$ or $v_r \gg 1$), i.e, in the low energy limit, the sojourn time in the above expressions tends to the Büttiker-Landauer traversal time for tunneling ($\tau_s^T \to \tau_{BL}$). Finally, regarding the local sojourn time in any part of the rectangular barrier, we find that the ratio of the time spent in the interval $[x_0, x_0 + A]$ to the time spent in the entire barrier is Δ/L, irrespective of x_0 in both the rectangular barrier as well as the S-dimer. We conclude that in these cases, the wave spends an equal amount of time in equal intervals of the barrier region.

3.3.3   The conditional sojourn time for reflection

Now, let us consider the sojourn time for reflection in the cases of the over-the-barrier propagation and sub-barrier tunneling. The sojourn time for reflection can be defined as for the case of transmission:

$$\tau_s^R(E > V_r) = \hbar\Delta/2 \lim_{\xi \to 0} \frac{\partial}{\partial \xi}[\ln|R(V_i = 0, \xi)|^2], \tag{3.20}$$

$$\tau_s^R(E < V_r) = i\hbar\Delta/2 \lim_{\xi \to 0} \frac{\partial}{\partial \xi} \ln[R(V_i = 0, \xi)/R^*(V_i = 0, \xi)]. \tag{3.21}$$

The reflection sojourn time for the general case of Fig. 3.4a straightforwardly works out as,

$$\frac{\tau_s^R(E > Vr)}{\tau_{BL}} = \frac{\tau_s^T(E > Vr)}{\tau_{BL}} + \frac{|r_{23}|^2 - |r_{21}|^2}{|r_{23}|^2 + |r_{21}|^2 - 2\Re(r_{21}r_{23}e^{ik_r L})} \tag{3.22}$$

This expression is not positive definite and in fact, becomes negative as we go across a transmission resonance ($|R| = 0$). In the case of tunneling, we obtain

$$\frac{\tau_s^R(E < Vr)}{\tau_{BL}} = \frac{\tau_s^T(E < Vr)}{\tau_{BL}} + \frac{|r_{23}|^2 e^{-2k_r L} - |r_{21}|^2 e^{2k_r L}}{|r_{23}|^2 e^{-2k_r L} + |r_{21}|^2 e^{2k_r L} - 2\Re(r_{21}^* e^{i\alpha}r_{23})}, \tag{3.23}$$

which is again not positive definite. In fact, even for the case of a symmetric rectangular potential, this time is negative.

Now, if we look at the partial wave expansions for the transmission and the reflection amplitudes in Equation(3.12), we would realize one difference between the transmission and the reflection. All the partial waves of the transmitted wave sample the region of interest and correspondingly pick up the paired combination $\xi = V_i \Delta$ in the amplitude, or the phase. In the case of reflection, however, there is one partial wave corresponding to the partial reflection from the front edge of the potential upto the region of interest (see Fig. 3.4), due to the element r_{12} in the partial wave expansion, that never samples the region of interest where the imaginary potential is applied. This part corresponds to the ***prompt*** part of the reflection. Arguably, if this partial wave never enters the region where the imaginary potential is applied, it should never have been affected by it and the weightage corresponding to this partial wave should be eliminated out of reckoning. But, it is clear from the above expressions that this partial wave interferes with the rest of the partial waves, and thus affects the time to be clocked spuriously. This problem can be overcome by explicitly removing this prompt part of the reflection. ~~This can be accomplished by setting $R \to R - r_{12}$ in Eqn.(3.12) in the 1D case.~~ Now we obtain the sojourn time ~~for reflection (for $E > V$ as well~~ as for $E < V_r$) as

This can be accomplished by explicitly removing the term r12 in the hand side of Eq. (3.12) in the 1D case.

$$\tau_s^R = \tau_s^T + \tau_{BL}. \tag{3.24}$$

The reflection time in this interpretation is the sum of the transmission time and a propagation time across the sub-interval. Consequently it is always greater than the transmission sojourn time. But now the reflection time is also positive definite. In fact, an experimental implementation of this procedure is also possible. One can cause the reflection from a modified potential whose reflection coefficient is equal to r_{12} to interfere destructively with the reflection from the potential in which we seek the sojourn time. For example, one can use the same potential but index matched to the continuum beyond from the point where the imaginary potential is applied (as shown in Fig. 3.4c) as the modified potential.

3.4 The reflection delay time in the WKB approach

The sojourn time problem can also be dealt with using the WKB wave function $\psi(x)$ [109] within the barrier region. Using the particle current density $j(x) =$
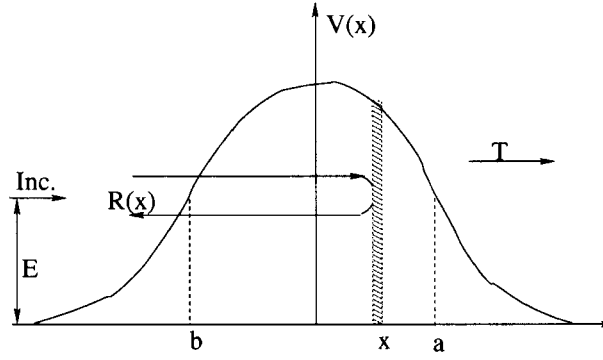
Figure 3.5: A schematic of the potential showing the classical turning points and the partial reflections in the WKB approach.

$(\hbar/2im)[\psi^*(d\psi/dx) - \psi(d\psi^*/dx)]$, the total velocity field $v(x)$ is given by the relation $j(\mathrm{x}) = v(x)\psi^*(x)\psi(x)$. Evaluating the total velocity field using the WKB wave function yields an expression [73] in which the total velocity field can be split into a sum of the forward velocity field and a backward velocity field. The forward velocity field is given by $v_f(x) = p(x)/m$, giving the traversal time as $\tau^T = \int_a^b m/p(x)\,\mathrm{d}x$, where a and b are the classical turning points and $p(x) = \sqrt{2m(V_r(x) - \mathrm{E})}$. This time is consistent with the Büttiker-Landauer time for a rectangular barrier. Using this, the reflection sojourn time for tunneling can be written as a properly weighted sum over the partial reflections from each point within the barrier (See Fig. 3.5) as (there is no multiple scattering here):

$$\tau^R = \int_b^a 2 \left[\int_b^x \frac{m\,dx'}{p(x')} \right] \frac{\mathcal{R}(x)\,dx}{\int_b^a \mathcal{R}(x)dx}, \qquad (3.25)$$

where $\mathcal{R}(x)$ is the (probability) reflection coefficient of the barrier extending from only x upto a, and in the WKB approximation is given by [110]

$$\mathcal{R}(x) = 1 - \exp\left[-2\int_x^a p(x'')/\hbar\,\mathrm{dx''}\right] . \qquad (3.26)$$

Using the above expression, we will now proceed to calculate the delay times for two symmetric potentials, *viz.*, the rectangular potential barrier of height V_r and width L, and a parabolic potential barrier $V(x) = -1/2\mathrm{w}^2\mathrm{x}^2$. For the rectangular barrier, we obtain the reflection delay time as

$$\tau^R = \frac{mL}{p_0 N} - \frac{m\hbar}{p_0^2 N} + \frac{2m}{p_0 N}\left(\frac{\hbar}{2p_0}\right)^2 \left(1 - e^{-2p_0 L/\hbar}\right), \qquad (3.27)$$

where $N = [1 + \hbar/2p_0 L(1 - e^{-2p_0 L/\hbar})]$ and $p_0 = \sqrt{2m(V_r - E)}$. We note that for a sufficiently wide barrier $p_0 L/\hbar \gg 1$ and the reflection time can be expanded in powers of $\hbar/p_0$. To the zeroeth order, $\tau^R = \tau^T = mL/p_0$, i.e., the reflection time is the same as the transmission time. In the case of the parabolic barrier, the transmission time is $\tau^T = \pi\sqrt{m}/\omega$ and the reflection time is

$$\tau^R = \frac{\pi\sqrt{m}}{\omega} + \frac{2\sqrt{m}}{\omega} \int_{-2E/\sqrt{\omega}}^{2E/\sqrt{\omega}} \frac{\sin^{-1}\left(\frac{\omega x'}{2E}\right) \mathcal{R}(x')\, dx'}{\int_{-2E/\sqrt{\omega}}^{2E/\sqrt{\omega}} \mathcal{R}(x')\, dx'} \tag{3.28}$$

where

$$\mathcal{R}(x) = 1 - \exp\left(\frac{-\pi E\sqrt{m}}{\hbar\omega}\right) \exp\left[\frac{2E\sqrt{m}}{\hbar\omega}\left(\frac{\omega x}{\sqrt{2E}}\sqrt{1 - \omega^2 x^2/2E} + \sin^{-1}(\omega x/\sqrt{2E})\right)\right] \tag{3.29}$$

$\mathcal{R}(x) \sim 1$ for a reasonably small w or a broad potential. Then the second part of the expression for τ^R is negligible, giving $\tau^R = \tau^T$. For $\mathcal{R}(x) < 1$, the reflection time is slightly lesser than the transmission time. But within the validity of the WKB approach, it appears that the reflection and transmission times are equal in this case also.

3.5   The case of the random potential

Coming now to the case of the random potentials, let us consider Eq.(3.13). The first part on the right hand side consisting of the diagonal terms represents mainly the growth of the wave, while the second part consists of the off-diagonal terms representing the interferences. For a disordered potential, we will expect the phases to be random, and for any typical configuration of the random potential, the off-diagonal terms to contribute very little. Thus, we do not expect the problem of the negative times for a random potential. Due to the random phases of the partial waves, the problem of the random potential becomes similiar to the classical diffusion problem. We will deal with the problem of the distribution of sojourn times from a random potential further in Chapter-4.

3.6   Conclusions

In conclusion, we have pointed out that the non-unitary clock involving the imaginary potential (iV_i) can lead to a negative sojourn time for non-random potentials. This

negativity can be traced to the 'spurious' scattering caused by the very clock potential introduced for clocking the sojourn time through coherent amplification/attenuation. A simple, formal mathematical procedure has been given to remove the effects of this spurious scattering. In the case of reflection, we further needed to remove the *prompt* part of the reflection. With these corrections, the sojourn times are positive definite, in general. We also find that the corrected non-unitary clock yields a sojourn time with the proper low-energy limit in agreement with the Buttiker-Landauer traversal time. We have also given an expression for the reflection delay time within the WKB approximation. It is also clarified why the problem of spurious scattering effectively does not arise for a random potential.

This problem of the 'clock' mechanism affecting the time to be clocked is not special to the non-Unitary clock alone. It also affects the Larmor clock [75] and possibly every clock where the perturbation due to the clock mechanism couples to the Hamiltonian. Indeed, we have explicitly verified the case for the Larmor clock and have found that the corrected Larmor times for traversal, τ_y and τ_z corresponding to spin precession and spin-rotation [75] are exactly our sojourn times for traversal in the case of propagation $(E > V_r)$ and tunneling $(E < V_r)$ respectively. Additionally, for the Larmor clock, there is a relation between the z-component of the spin of the transmitted and the reflected waves due to conservation of angular momentum. This makes it difficult to define separate conditional reflection and transmission times using the spin-rotation (τ_z).

The problem of negative conditional sojourn times calculated by different procedures has been noticed by several authors, notably Golub *et al.* [79], Buttiker *et al.* [111] and Hauge and Støvneng [68]. Golub *et al.* [79], while proposing that absorption could act as a clock, noticed that the scattering due to mismatch in the clock potential would affect the performance of the clock, but decided that conditional sojourn times might not make any sense. The sojourn time is a useful conceptual tool and the sojourn time, defined in our sense as more of an interaction time, should not only be real [68], but positive definite as well in order to be physically meaningful. Any other quantity, though experimentally meaningful, such as the precession of a spin in a magnetic field, cannot be interpreted as the time of sojourn, unless it yields a positive definite quantity. Coming to the experimental implementation of

the corrected non-unitary clock, it can be readily realized, in principle, in electron tunneling through a mesoscopic barrier as absorption through fake channels (inelastic electron-electron or electron-phonon scattering processes), where only the coherent part of the transmitted/reflected wave is measured by an interference detection.

The main problem in defining a meaningful sojourn time for a quantum system is because of interference between partial waves (the alternatives) that defies naive realism or objectification of the alternatives. Thus, it is clear that there exists no self-adjoint operator in quantum mechanics for the sojourn time and it is not an observable[64]. But it is a calculable intermediate quantity (like a matrix element for a transition), which is practically useful for calculating other quantities, and for deciding for or against certain conditions. For example, in a given mesoscopic device, we would need to compare the dephasing/decoherence time to the time of sojourn in order to see if the dephasing would affect device performance. We view our correction of the quantum clock in this spirit. For example, when we suppress the prompt part of the reflection while calculating the reflection time, we take the view that the partial waves corresponding to the prompt part would never sample that region where there is dephasing, in order to get affected by it. To re-emphasize, in order for the sojourn time to be a conceptually and practically useful tool, we require a prescription which yields a sojourn time which is (i) real, (ii) positive, (iii) additive (time spent so calculated for different parts should add up to give the total time), (iv) calculable, (v) measurable, even if not observable as an operator in quantum mechanics, and (vi) it should causally relate to the region of interest, *i.e.*, the partial waves should have traversed that region. Hopefully, we have provided such a prescription here, in that the sojourn time so calculated has the above properties. It only helps matters that the experimental realization of this procedure is possible in principle.